SPATIO-TEMPORAL ANALYSIS OF WULAN DELTA IN INDONESIA: CHARACTERISTICS, EVOLUTION, AND CONTROLLING FACTORS

Bagus SEPTIANGGA[1], Bachtiar W. MUTAQIN[2*]

DOI: 10.21163/GT_2021.163.04

ABSTRACT:
The evolution of the Wulan Delta began after the construction of the Wulan River Canal in 1892. It alters the shoreline erosion and accretion that affect the land dynamics of the coastal area. This study aims to analyze the spatio-temporal evolution of the Wulan Delta, including the shoreline and its dynamics, as well as the geomorphological processes that affect it. The shoreline change was extracted digitally from Landsat satellite images and divided into four periods, i.e., 1995-2000, 2000-2011, 2011-2015, and 2015-2020. We used the histogram thresholding method to separate the land from the sea and produce the shoreline as the interface. This research employed field check and focus group discussion for identifying the cause and impact of shoreline dynamics in the research area. The results show that land loss and accumulation over 25 years (1995-2020) are -7.16 km^2 and +6.58 km^2, respectively. In Wulan Delta, the erosion is due to high waves and sedimentation due to mangrove planting and high sediment from the rivers. The development rates of the Wulan Delta for the period of 1995-2020 were 73,200 m^2/year.

Key-words: *coastal, morphodynamics, histogram thresholding, Wulan Delta, Indonesia.*

1. INTRODUCTION

The coastal area has high productivity of available resources and an essential role in supporting human lives (UNISDR/UNDP, 2012; Mutaqin, 2020; Marfai et al., 2020; Mutaqin et al., 2020). Hence, the coastal area is essential for human existence since almost all major cities are located in this area. Furthermore, one-third of the world population was living in the coastal area, and the numbers always increase year by year. This situation can inflict an increasing hazard level in the coastal areas since this area is very dynamic due to its natural and human processes (Mujabar and Chandrasekar, 2013; Mutaqin, 2017; Mutaqin et al., 2019; Arjasakusuma et al., 2021).

Delta evolutions due to sedimentation are one example of the dynamics phenomenon in the coastal area (Chen et al., 2020; Collins et al., 2021). Wulan Delta (**Fig. 1**), as one of the most dynamics delta in Indonesia, has been experiencing rapid evolutions since the construction of the Wulan Canal in 1892 (Bird and Ongkosongo, 1980; Fadlillah et al., 2018; Fadlillah et al., 2019). The canal dredging generates intensive sedimentation that is transported through the Serang River and deposited in the estuarine. This condition has accelerated the formation and evolution of the Wulan Delta. As Fadlillah et al. (2018) state, aside from massive sediment transport, human construction in aquaculture and housing on Wulan Delta's body also contributes to its development, including its water environment. Although the tidal patterns in Wulan Delta are categorized as micro-tidal with a mean of 0.8 m, flat morphology in this area leads to the tidal run-up that can reach far ashore, up to 8 km upstream during floods, and in other hands also making this area as an area which vulnerable to sea-level rise (Marfai, 2014; Fadlillah et al., 2019). The evolution of the Wulan Delta provides several benefits to the local community. The community has utilized a broader land in Wulan Delta to build fishponds. Furthermore, the local community also competes to mark the new lands emerging in the estuarine during low tides to be recognized as their own (Ruswanto and Adisaputra, 1990). Simultaneously, several settlements and fishponds in three villages in the north of Wulan Delta (Semat, Tanggultlare, and Bulak Village) have been destroyed and sink in due to the erosion. Most residents in that three

[1]*Ministry of Public Works and Housing, Directorate General of Water Resources, Jakarta, Indonesia, septianggabagus@gmail.com*
[2] *Universitas Gadjah Mada, Faculty of Geography, Coastal and Watershed Research Group, 55281 Yogyakarta, Indonesia, mutaqin@ugm.ac.id*

villages were forced to move, about 250-m inland from their previous settlements. In 1984, some of the remaining buildings, e.g., houses, mosques, and water reservoirs, were still seen. However, in 1993 all of the buildings were disappeared due to erosion (Ruswanto and Adisaputra, 1990).

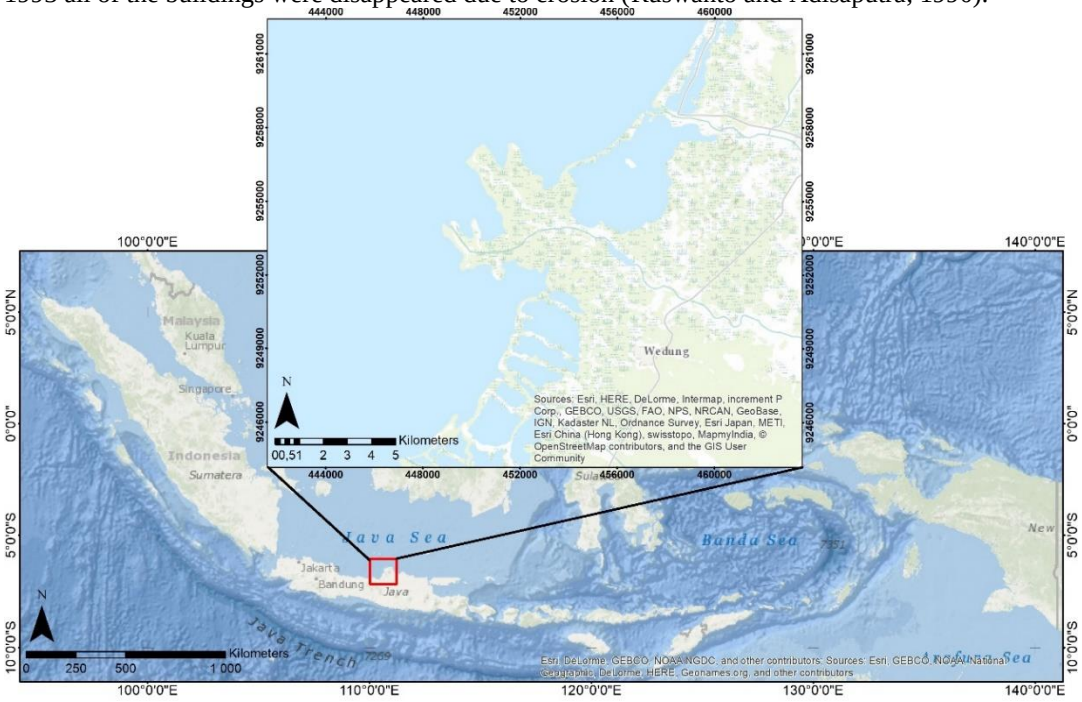

Fig. 1. Wulan Delta, one of the most dynamics delta in Indonesia.

Sunarto (2005) has described Wulan Delta's morphology from 1925 to 1992; Wulan Delta's dynamics are further analyzed in this study, i.e., from 1995 to 2020. Marfai et al. (2016) also has explained the Wulan Delta's morphodynamics but focuses more on social impacts. Furthermore, this study aims to analyze the spatio-temporal evolution of the Wulan Delta, including the shoreline and its dynamics, as well as the geomorphological processes that affect it. The research results in the form of the spatio-temporal map of Wulan Delta during 1995-2020, calculation of land loss and land accumulation, as well as the assessment of the annual rate of the Wulan Delta evolutions, can use as an input for disaster mitigation strategy in this area and its surroundings.

2. DATA AND METHODS

2.1. Laboratory and computational analysis

We used multi-temporal images of Landsat 5 TM (1995, 2000, and 2011) and Landsat 8 OLI/TIRS (2015 and 2020) from USGS (https://earthexplorer.usgs.gov/) as the database to recognize the evolution of Wulan Delta (**Table 1**). The spatio-temporal monitoring in the coastal area using remote sensing data could help understand the erosion distribution and quickly predict coastal evolution trends with extensive coverage area (Wahyunto et al., 1995; Cracknell, 1999; Zhang, 2011; Mutaqin, 2017; Wicaksono and Wicaksono, 2019; Costantino et al., 2020; Arjasakusuma et al., 2021).

Under normal conditions, the water favorably reflects the green wavelengths, i.e., Band 2 on Landsat 5 TM and Band 3 on Landsat 8 OLI/TIRS. The water also absorbs the energy at wavelengths that are longer than near-infrared. Near-infrared (Band 4 on Landsat TM and Band 5 on Landsat OLI/TIRS) is very well known in shoreline analysis since it distinguishes water from land (Tong et al., 2014; Al-Mansoori and Al-Marzouqi, 2016; Pardo-Pascual et al., 2018; Zhang and Hou, 2020). Therefore, this research's band ratios were 2/4 for Landsat TM and 3/5 Landsat OLI/TIRS. We used several steps to get better results during the satellite image processes (e.g.,interpretation and analyses),

such as image cropping, radiometric correction, histogram thresholding, and mean erosion distance (MED). We used Dark Object Subtraction (DOS) technique to fix the images' visual quality and fix the pixel values that did not correspond to the reflection values for radiometric image correction. This technique assumes that the digital value of the darkest objects on the Earth's surface is zero.

Table 1.

The types of satellite images used in this research.

Images	Censors	Paths/rows	Time acquired		Resolution (m)
			Dates	Clock	
Landsat 5	TM	120/65	May 22, 1995	13:55	30
Landsat 5	TM	120/65	July 6, 2000	14:24	30
Landsat 5	TM	120/65	June 19, 2011	14:37	30
Landsat 8	OLI/TIRS	120/65	June 14, 2015	14:47	30
Landsat 8	OLI/TIRS	120/65	August 30, 2020	14:48	30

The shoreline information was identified digitally based on the satellite images' pixel values (Maglione et al., 2017; Zhang and Hou, 2020). The identification used ENVI 4.7 software with the assistance of histogram threshold feature on interactive stretching (**Fig. 2a**). Histogram thresholding is the process of separating land from the sea-based on pixel values. The thresholding includes dividing the histogram into two visually separated parts by graphical valleys seen in the histogram (Marfai et al., 2008; Aedla et al., 2015; Nassar et al., 2018; Ghorai and Mahapatra, 2020). Moreover, the tabulated histogram is described of frequency distributions, and to interpret land and water from it, a density slice was applied. Thresholding was done by shifting the line threshold step by step until the gap between water (max value) and land (min value) was reached minimum gap and feature distinction were clear (Tong et al., 2014). The thresholding results are binary images that have two values; value 0 for water and value 1 for land. These images are processed further to generate a shoreline. This histogram separation produces a minimum value that indicates the water body and a maximum value that indicates land. Pixel values from thresholding separation for each image have been generated, as shown in **Table 2** that inform pixel values (minimum and maximum) for each feature. Moreover, the maximum water value gap and the minimum land value are where shorelines potentially emerge.

Table 2.

Pixel value for each feature.

Images	Year	Water threshold		Land threshold	
		Min	Max	Min	Max
Landsat 5 TM	1995	0.552	0.792	0.795	2.896
Landsat 5 TM	2000	0.074	0.527	0.530	3.926
Landsat 5 TM	2011	0.194	0.519	0.521	3.500
Landsat 8 OLI/TIRS	2015	0.552	0.743	0.744	2.670
Landsat 8 OLI/TIRS	2020	0.554	0.749	0.751	2.625

The shoreline erosion and accretion from 1995 to 2020 were identified using the image processing method results, which were performed and analyzed quantitatively with the Mean Erosion Distance (MED) technique. With the MED technique, we also can obtain and determine the average land loss and land accumulation in the research area. The scenario and the equation used in MED are shown in **Fig. 2b** and **Eq. 1**. The MED equation used in shoreline monitoring was according to Tong et al. (2014). The spatio-temporal evolutions of the Wulan Delta were identified quantitatively from the equation and then analyzed in a qualitative descriptive manner.

To determine the processes that occurred in the shoreline, we establish four sections as an observed shoreline based on the existing main processes. Sections A and D were selected to identify the primary morphodynamics processes and their influence on the Wulan Delta evolution. In contrast, Sections B and C were selected to determine the evolution of the delta. The section analysis aimed to obtain detailed information on the processes occurring in each section.

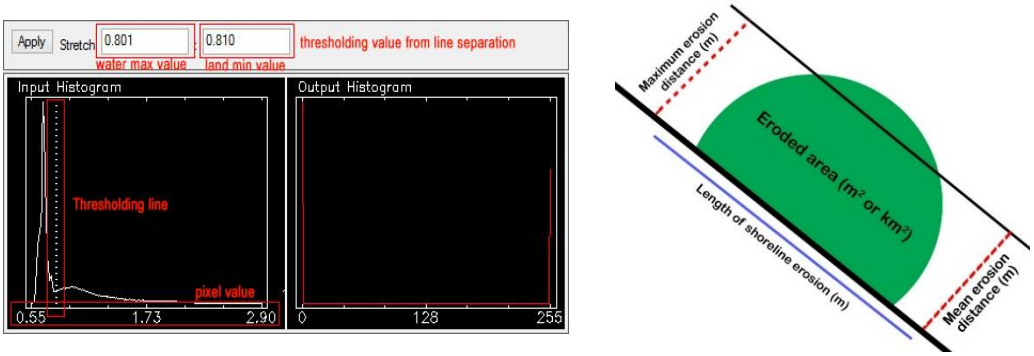

(a) (b)

Fig. 2. (a) An example of a histogram thresholding technique to separate the land and the water; and (b) Mean Erosion Distance (MED) scenario.

$$\text{Mean Erosion Distance (m)} = ES/L \quad (1)$$

where: ES -eroded or accreted area (m^2);
L -length of shoreline erosion/accretion (m)

2.2. Field observations

We conduct a Focus Group Discussion (FGD) with the local community, especially the fishpond owners in Wulan Delta and its surrounding areas (**Fig. 3a**). The FGD aimed to gather the information and identify the cause and impact of the erosion and accretion in the Wulan Delta according to the local communities' perspectives through a discussion. Furthermore, validation of shoreline extraction results has been done during field observations by ground checking for some sample points to prove the existence of morphodynamics processes that occur by looking for evidence (**Fig. 3b**).

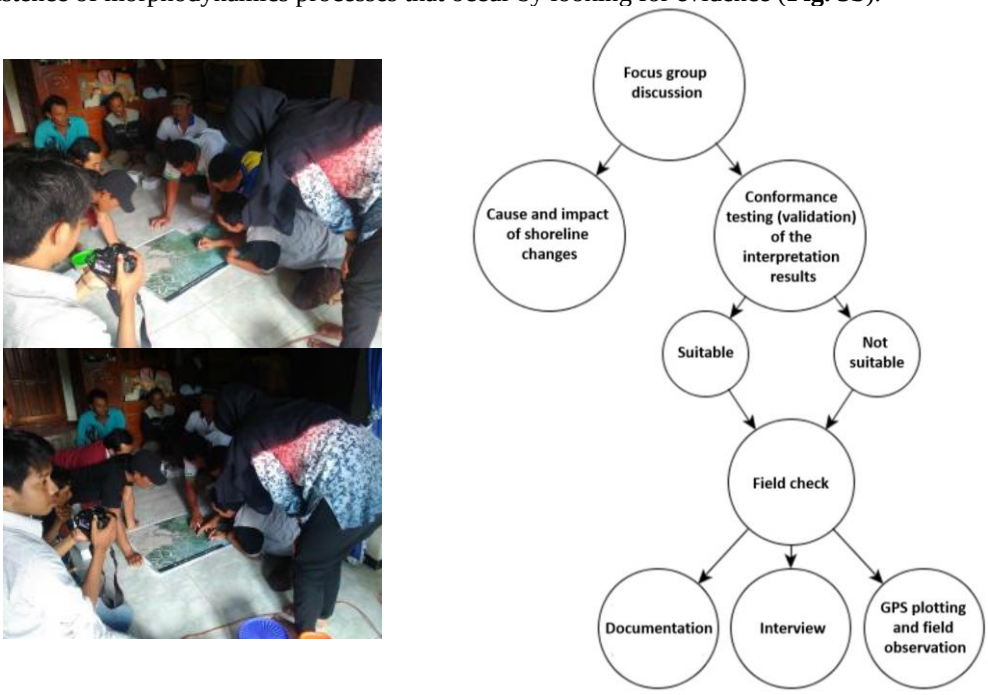

(a) (b)

Fig. 3. (a) Focus Group Discussion with the local community in Wulan Delta; and (b) Validation of shoreline extraction results during field measurements.

3. RESULTS AND DISCUSSIONS

3.1. Shoreline change

Detailed monitoring can show a clear description of the morphodynamics processes along the shoreline. As mentioned before, we divided the study area into four sections (A, B, C, and D). Section A consists of Purworejo, Betahwalang, and Wedung Village; Section B consists of Berahan Kulon Village; Section C consists of Berahan Kulon and Berahan Wetan Village; and Section D consists of Kedungmalang, Kalianyar, Surodadi, Panggung, Bulakbaru, and Tanggultlare Village. This research divided the years 1995-2020 into four periods, namely 1995-2000, 2000-2011, 2011-2015, and 2015-2020. During 1995-2000, the shoreline in the study area shifted both seaward and landward (**Fig. 4a**). We used 11 years (from 2000 to 2011) due to limited data available on the website of the United States Geological Survey (USGS). The year 2005 was initially a time limit in the second period. However, the only available 2005 image was from Landsat 7 ETM+, which experienced a string. A string is a malfunction appearing in the image pixels, resulting in diagonal black stripes on the image. Even though the string is repairable, the pixel value correction is not good enough for shoreline extraction. Moreover, the diagonal black stripes are also found on Landsat 7 ETM+ images from 2005 to 2010. Therefore, this research used the 2011 image of Landsat 5 TM as a substitute.

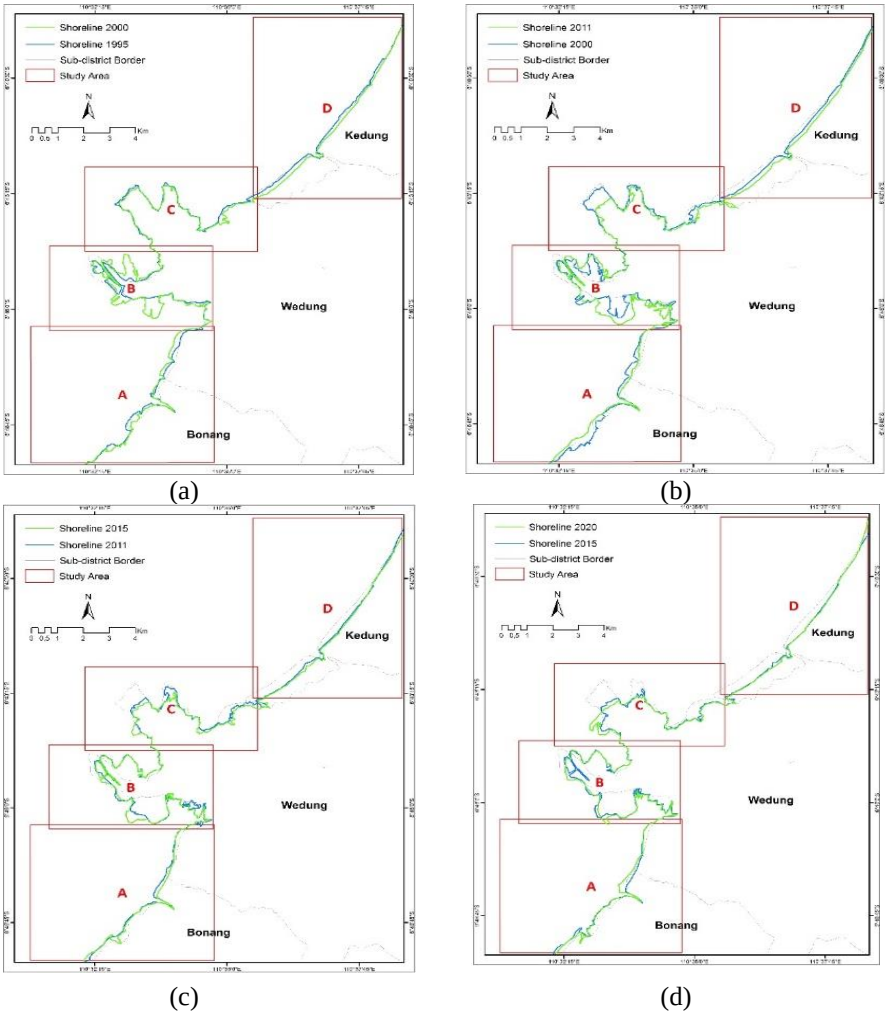

Fig. 4. The shoreline changes in Wulan Delta and its surrounding area during: (a) 1995-2000; (b) 2000-2011; (c) 2011-2015 and (d) 2015-2020.

The shoreline change analysis during 2000-2011 (**Fig. 4b**) used the same regional section as the analysis during 1995-2000. The shoreline change during 2011-2015 (**Fig. 4c**) was most significant than the shoreline change in the previous years or during 2015-2020 (**Fig. 4d**). This is due to the less deposited shoreline length during 2011-2015 (17.76 km) compared to other years, i.e., between 22.98-29.83 km. The shoreline change rate in this area during 25 years is more significant than what has happened in Yogyakarta and East Java (Mutaqin, 2017; Arjasakusuma et al., 2021).

Field observation was done by selecting 11 sample points (**Fig.5**) based on the most dynamic process that has occurred. Furthermore, this observation ensures the process generated from the laboratory by taking documentation and field observation. Locals accompanied this checking, so a locals interview was also conducted along with the observation to emphasize the results. According to Fadlillah et al. (2018), fishponds are the most dominant landuse; they expanded from 82.94% (2008) to 91.55% (2016) of major landuse in the Wulan Delta. Field observation strengthens this claim, and our observation found that from 11 ground points, 8 points were fishponds predominantly (**Table 3)**. In addition, Mangrove plants were also found in 9 out of 11 points. As Marfai et al. (2016) assert that Wulan Delta morphodynamic causes landuse conversion from mangroves to fishponds; this condition will continue to happen in the future due to the extent of mangrove vegetation and fishponds as a local primary livelihood source.

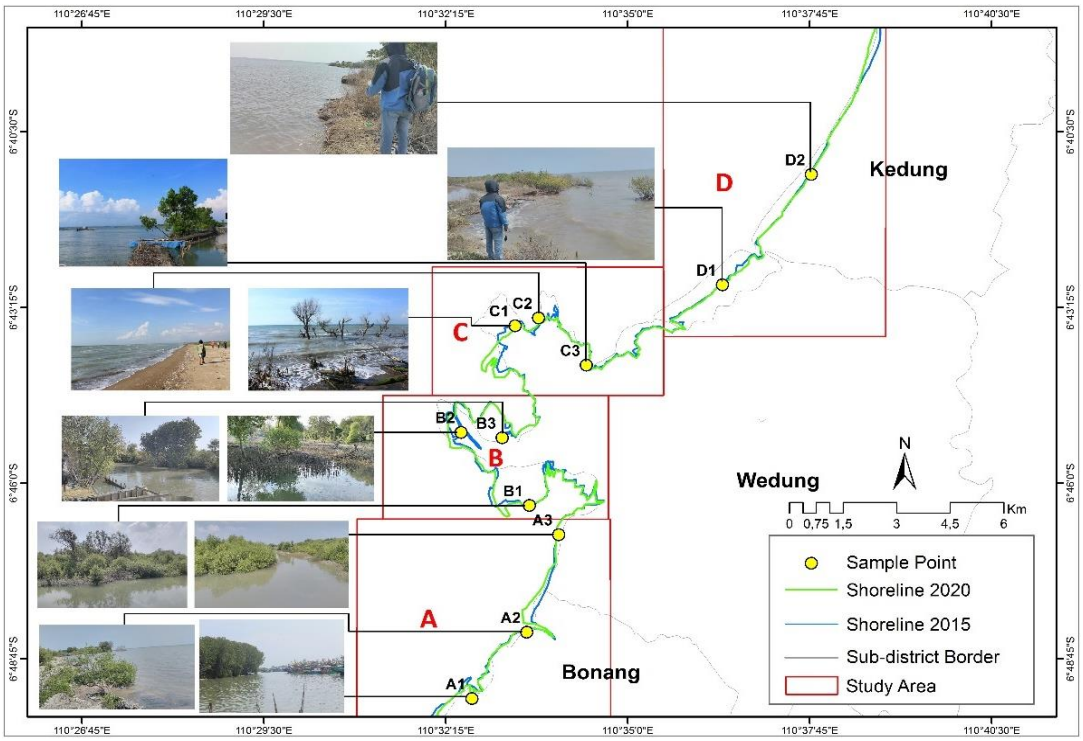

Fig 5. Field observation samples to ensure the process generated from laboratory.

Based on local explanation through focus group discussion (**Table 4)**, shoreline deposition on points A1 and A2 was caused by mangroves planting along the coast around the 2000s. Meanwhile, at point A3, there has been erosion since the 2000s and caused many fishponds to be damaged, and it was proven by the remains of wooden stakes near the shore. All sample points in area B show the land deposition process due to the massive sediment load from the Wulan River. According to the locals (**Table 4)**, accretion has been going for a long time, and the mangrove zone has made the accretion faster and often triggers land ownership conflicts. There have been deposition in points B1,

B2, and B3, which began to form around 1990. Moreover, calm waves make the process more dominant and faster.

Table 3.

Validation result from field observation and interview.

Sample point	Dominant process (tentative map)	Interview validation		Vegetation	Land use
		Process	Note		
A1	Deposition	Confirmed	The deposition had occurred since the 2000s	Mangrove	Fishpond, settlement, port
A2	Deposition	Confirmed	The little deposition had occurred since the 2000s	Mangrove	Fishpond
A3	Erosion	Confirmed	Erosion had occurred since the 2000s	Mangrove	Fishpond
B1	Deposition	Confirmed	The massive deposition has occurred since 1990	Mangrove	-
B2	Deposition	Confirmed	The massive deposition has occurred since 1990	Mangrove	Fishpond
B3	Deposition	Confirmed	The massive deposition has occurred since 1990	Mangrove	Fishpond
C1	Erosion	Confirmed	Massive erosion has occurred since the 1990s	Mangrove	-
C2	Erosion	Confirmed	Massive erosion has occurred since the 1990s, emergence of spit landforms in early 2000	-	Empty land
C3	Erosion	Confirmed	Erosion has occurred since the 2000s	Mangrove	Fishpond
D1	Erosion	Confirmed	Erosion has occurred before 1995	Mangrove	Fishpond
D2	Erosion	Confirmed	Erosion has occured before 1995	-	Fishpond

Table 4.

Focus Group Discussion (FGD) result.

Sample point	Process confirmed	Focus Group Discussion		
		Cause	Effect	Local adaptation
A1	Deposition	Mangrove planting	New land	New land used for fishponds
A2	Deposition	Mangrove planting	New land	New land used for fishponds
A3	Erosion	High waves	Fishponds damage	Mangrove planting
B1	Deposition	Calm waves, sediment from the river	New land, land claim conflict	New land used for fishponds
B2	Deposition	Sediment from river	New land, land claim conflict	New land used for fishponds
B3	Deposition	Calm waves, sediment from the river	New land, land claim conflict	New land used for fishponds
C1	Erosion	High waves	Mangrove damage	Mangrove planting
C2	Erosion	High waves	The emergence of the natural barrier since the 2000s	Mangrove planting
C3	Erosion	High waves	Fishponds damage	Mangrove planting
D1	Erosion	High waves	Fishponds damage, irregular beach	Build shore protector from wood
D2	Erosion	High waves	Fishponds damage, irregular beach	Build shore protector from wood

Point C1 is located in the forefront area at the delta's foot and directly faces the open sea. Large waves have caused this area to experience shoreline erosion from 1995 until now. In addition, massive

damage to mangrove plants and fishponds has also occurred in this area. Point C2 is the location of Spit landform, and according to the local community (**Table 4)**, it is also called 'Tirang', which stretches like an arrow along the coast around delta's foot, and it emerged around the 2000s. This landform becomes a natural barrier to prevent further erosion. Uniquely, this landform stretch and covers seawater trapped on the land and formed a lagoon. Likewise, Point C3 has experienced erosion since the 2000s and damaged many fishponds. The shoreline erosion in area D also continues from 1995 until these days. However, the shoreline retreat is not as intensive as before because the community started to make wave protectors from wood along the shore. Shoreline erosion at points D1 and D2 caused irregular shoreline form. The erosion makes the community's fishponds continue to be threatened, whereas aquaculture is still the local communities' main livelihood.

3.2. Land loss and land accumulation

The morphodynamics assessment emphasizes more on land loss and land accumulation during 1995-2020. According to Sunarto (2005), Wulan Delta experienced positive growth continuously from 1925 to 1995. It changed from 1.9 km^2 to 9.15 km^2 over 70 years at a growth rate of 0.39 km^2/year. Shoreline change accompanied the evolution during 1995-2020 on the south and the north of the delta. The land loss and land accumulation in the south varied uniquely. However, the coastal area on the north experienced land loss progressively.

The morphodynamics map, which shows the land loss and land accumulation in Wulan Delta and its surroundings during 1995-2020, is presented in **Fig. 6**. The map shows land loss distribution and land accumulation in 1995-2000, 2000-2011, 2011-2015, and 2015-2020. Aside from land loss and land accumulation, this map provides information on mean distance erosion and deposition, which are useful for determining the average distances of shoreline retreats and advances. **Table 5** shows the land development and mean erosion or deposition distance.

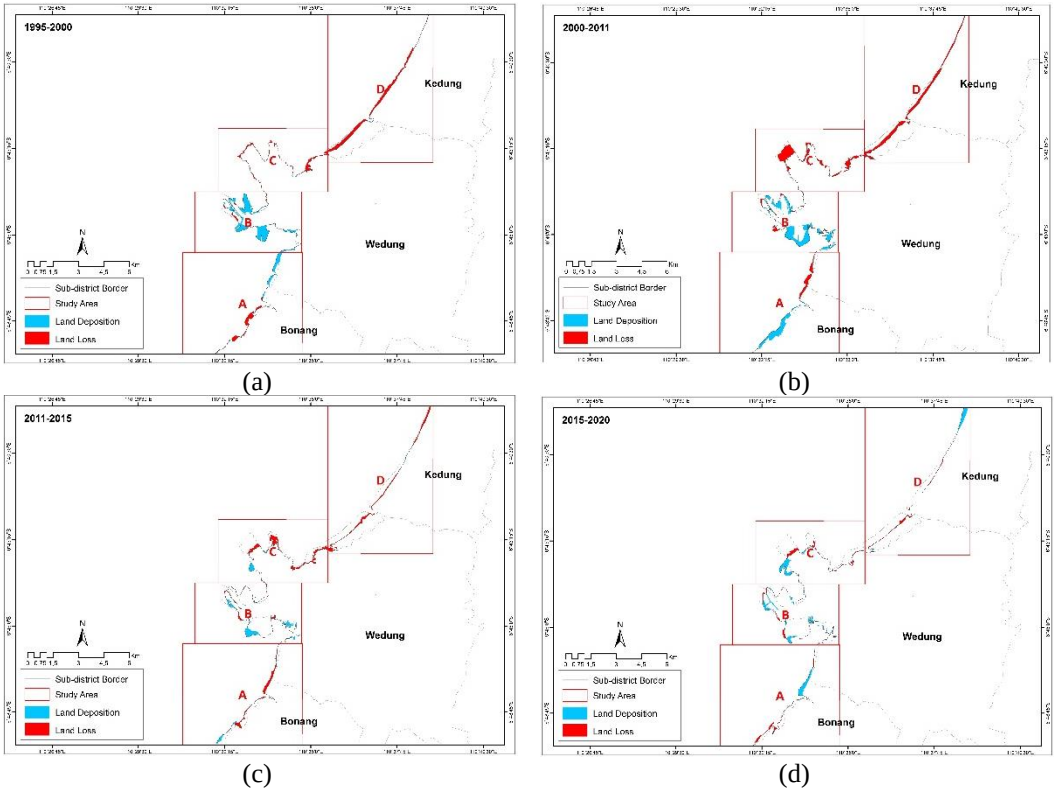

Fig. 6. Map of the spatio-temporal evolution of Wulan Delta and its surrounding during: (a) 1995-2000; (b) 2000-2011; (c) 2011-2015; (d) 2015-2020.

The shoreline in Section-A experienced moderate land loss during 1995-2000, i.e., 0.35 km^2, and continuously increased until the period of 2011-2015, which reach 0.38 km^2. However, the land loss had declined in the following years, i.e., 0.18 km^2 in the period of 2015-2020. Meanwhile, this section's shoreline accretion fluctuated and peaked during 2000-2001, causing the most massive land accumulation, i.e., 0.71 km^2. Coastal erosion leads to shoreline retreats by an average of 64.76 m. Meanwhile, due to accretion, the shoreline shifts with an average as far as 68.24 m seaward.

The land loss and the land accumulation in Section-B are imbalanced. Land accretion tends to be higher since it is located in the river estuary (Arjasakusuma et al., 2021). The most extensive land accumulation was 1.62 km^2 during 2000-2011, whereas the severest land loss was 0.16 km^2 during 2000-2011 and 2011-2015. The shoreline in this section has retreated by an average of 24.29 m and advanced by 72.12 m.

Table 5.

Morphodynamics and the mean erosion or deposition distances in Wulan Delta and its surroundings.

Sections	Periods	Morphodynamics (km^2)		Eroded shoreline length (km)	Deposited shoreline length (km)	Mean erosion distance (m)	Mean deposition distance (m)
		Land loss	Land deposition				
Section A	1995-2000	-0.35	0.38	-4.15	6.63	84.34	57.32
	2000-2011	-0.36	0.71	-3.99	6.76	90.23	105.03
	2011-2015	-0.38	0.09	-7.32	2.18	51.91	41.28
	2015-2020	-0.18	0.33	-5.53	4.76	32.55	69.33
Section B	1995-2000	-0.09	1.57	-3.51	12.69	25.64	123.72
	2000-2011	-0.16	1.62	-5.33	18.23	30.02	88.86
	2011-2015	-0.16	0.54	-12.66	11.57	12.64	46.67
	2015-2020	-0.15	0.49	-5.20	16.76	28.85	29.24
Section C	1995-2000	-0.44	0.02	-11.49	2.03	38.29	9.85
	2000-2011	-1.11	0.01	-12.45	1.24	89.16	8.06
	2011-2015	-0.57	0.13	-9.81	2.75	58.10	47.27
	2015-2020	-0.27	0.35	-8.03	4.32	33.62	81.02
Section D	1995-2000	-0.99	0.02	-9.95	1.63	99.50	12.27
	2000-2011	-1.22	0.00	-12.75	0.00	95.69	0.00
	2011-2015	-0.55	0.01	-11.49	1.26	47.87	7.94
	2015-2020	-0.18	0.31	-17.72	3.99	10.16	77.69

A contrary phenomenon has been found in Section-C, where the land loss was dominant. Shoreline erosion created a land loss of 2.39 km^2 over 25 years, whereas the land deposition reaches 0.51 km^2 with the highest land accretion is 0.35 km^2 during 2015-2020. The length of the shoreline in Section-C continues to decline. The shoreline in this section has retreated with an average of 54.79 m and advanced by 36.55 m. The land loss in Section-D, lying administratively on Jepara Regency, is the most severe. Over 25 years, total land loss in this section reaches 2.94 km^2, with the most significant land loss was during 2000-2011, which reach up to 1.22 km^2. Meanwhile, the most massive land accumulation was only 0.31 km^2 during 2015-2020. The severe land loss reduces the length of the shoreline in Section-D progressively. On average, the shoreline in this section has retreated by 63.31 m and advanced merely by 24.46 m.

The shoreline morphodynamics was analyzed comparatively with the wind and wave data of Demak and Jepara. The analysis aimed to identify the relationship between the cause and impact of the shoreline with the coastal morphodynamics.

Wind speed and direction influence the direction and magnitude of sea waves proportionally. During the west monsoon, the wind speed tends to become stronger, and the wave tends to become higher and more destructive (Muskananfola et al., 2020). This situation is different from the southern part of Java, where the high and extreme waves happened during the east monsoon (Mutaqin, 2017). Destructive waves erode the shoreline in Demak and Jepara (Muskananfola et al., 2020). On the contrary, during the east monsoon, the wind speed tends to be weaker, and the wave tends to be lower.

The intensity of the eastern sea wave is reduced by Muria Peninsula, causing land accretion along Demak and Jepara's shoreline.

The local community's adaptation is more to structural adaptation, such as making protective stakes and mangrove planting. Despite the loss, the positive side has been obtained by the fishermen. Fishers in area C are lucky because they can build the floating fish cage close to the beach because of the coastal erosion process, this evidenced by the discovery of several floating fish cage in area C.

3.3. Evolution of Wulan Delta

The delta initially had grown into a straight shape (strand plain) before it developed into a bird-foot shape (digitate). According to Setiawan (2014), the shoreline accretion in Wulan Delta is due to Muria Volcano's presence that supplies abundant obsolete materials to the Wulan River. As a result, the Wulan River estuary experiences progradation continuously, and the Wulan Delta area widens. **Fig. 7** shows Wulan Delta's development from 1995 to 2020, which also depicts image interpretation and field survey results.

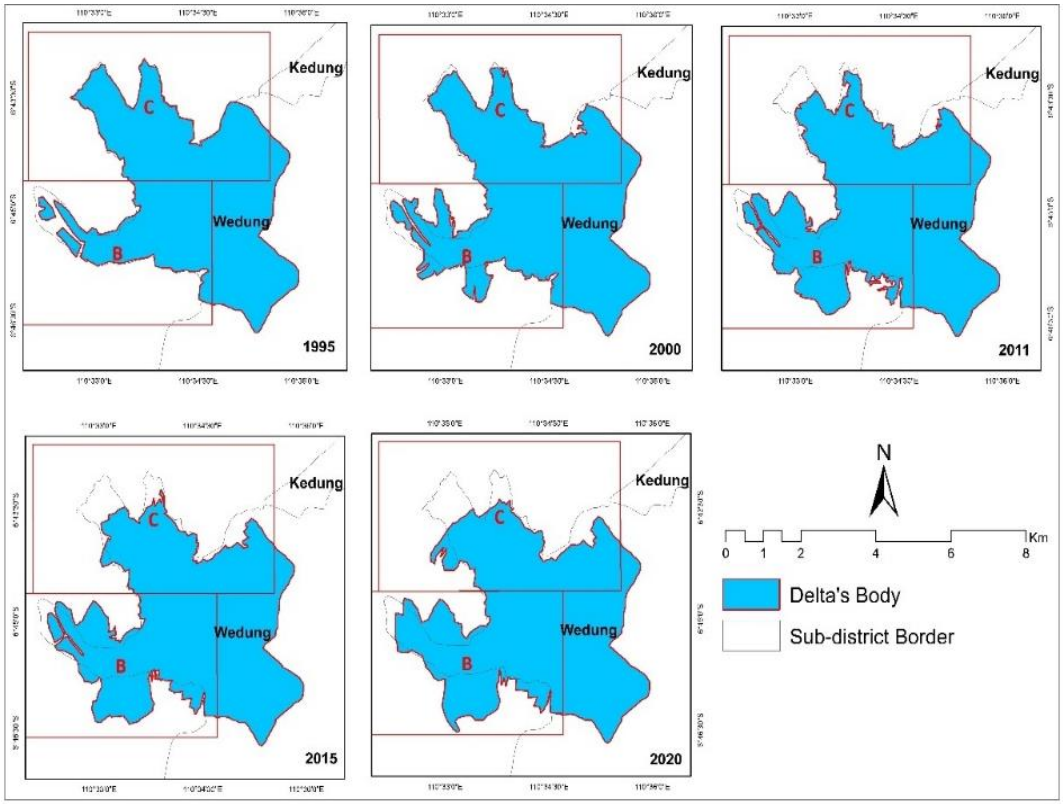

Fig. 7. The development of Wulan Delta during 1995–2020.

Wulan Delta has a bird-foot shape because the Wulan River bifurcates into two rivers, i.e., northward and northwestward, causing shoreline accretion to occur on these two distributary channels. Also, these river channels develop differently. According to Sunarto (2005), the main development initially occurred on the northwestern channel. However, in 1972, the northern channel began to form. Therefore, the shape of the delta changes to arcuate, cuspate, and digitate. Based on the Wulan Delta development presented in **Fig. 7**, we identify the extensive development and delta growth rate during 1995-2020 (**Table 6**).

Table 6.

The development and the growth rate of Wulan Delta during 1995 – 2015.

Years	Size of Delta (km^2)	Total growth (km^2)	Growth rate (km^2/year)	Growth percentage (%)
1995	21.19	-	-	-
2000	22.27	1.08	0.216	4.85
2011	22.62	0.35	0.032	1.55
2015	22.60	-0.02	-0.005	-0.09
2020	23.02	0.42	0.084	0.02

The Wulan Delta area always experienced extensive accumulation during 1995-2020, as seen in **Table 6**. It accumulated from 21.19 km^2 in 1995 to 23.02 km^2 in 2020. The most extensive land growth over 25 years happened during 1995-2000, which reach 1.08 km^2. It was enormously more significant than the land growth during 2011-2015 since the Wulan Delta area was reduced by 0.02 km^2. The growth rate in **Table 6** was obtained from the division of total growth by the length of the period. The highest growth rate was during 1995-2000, i.e., 216,000 m^2/year, while the lowest one was during 2011-2015, i.e., 5,000 m^2/year. The growth percentage describes the percentage of accumulated land to the total area of the Wulan Delta. It is proportional to total growth.

4. CONCLUSIONS

Over the years of 1995-2020, the shoreline change in Wulan Delta and its surroundings varied widely. An inconsistency is found in the southern part of the delta, representing shoreline retreats and advances. However, the shoreline continuously retreats in the northern part of the delta due to high waves. Wulan Delta has divided into two parts, i.e., southern and northern, which experience various changes. The northern shoreline retreats, while the southern one advances due to mangrove planting and high sedimentation from the rivers. During 1995-2020, the total land loss and accumulation in the study area were -7.16 km^2 and +6.58 km^2, respectively. The growth rates of the Wulan Delta over 25 years (1995-2020) were 73,200 m^2/year.

R E F E R E N C E S

Aedla R., Dwakarish G.S., Reddy D.V. (2015). Automatic Shoreline Detection and Change Detection Analysis of Netravati-GurpurRivermouth Using Histogram Equalization and Adaptive Thresholding Techniques. *Aquatic Procedia*, 4, 563-570. https://doi.org/10.1016/j.aqpro.2015.02.073.

Al-Mansoori S. and Al-Marzouqi F. (2016). Coastline Extraction using Satellite Imagery and Image Processing Techniques. *International Journal of Current Engineering and Technology*, 6(4), 1245-1251.

Arjasakusuma S., Kusuma S.S., Saringatin S., Wicaksono P., Mutaqin B.W., Rafif R. (2021). Shoreline Dynamics in East Java Province, Indonesia from 2000 to 2019 Using Multi-sensor Remote Sensing Data. *Land*. 10(2), 100. https://doi.org/10.3390/land10020100.

Bird E., and Ongkosongo O.S.R. (1980). *Environmental Changes of the Coasts of Indonesia*. Tokyo: United Nations University. 510p.

Chen D., Li X., Saito Y., Liu J.P., Duan Y., Liu S., Zhang L. (2020). Recent evolution of the Irrawaddy (Ayeyarwady) Delta and the impacts of anthropogenic activities: A review and remote sensing survey. *Geomorphology*, 365, 107231. https://doi.org/10.1016/j.geomorph.2020.107231.

Collins D.S., Nguyen V.L., Ta T.K.O., Mao L., Ishii Y., Kitagawa H., Nakashima R., Vo T.H.Q., Tamura T. (2021). Sedimentary evolution of a delta-margin mangrove in Can Gio, northeastern Mekong River delta, Vietnam. *Marine Geology*, 433, 106417. https://doi.org/10.1016/j.margeo.2020.106417.

Costantino D., Pepe M., Dardanelli G., Baiocchi V. (2020). Using Optical Satellite and Aerial Imagery for Automatic Coastline Mapping. *Geographia Technica*, 15(2), 171-190. http://doi.org/10.21163/GT_2020.152.17.

Cracknell A.P. (1999). Remote Sensing Techniques in Estuaries and Coastal Zones. *International Journal of Remote Sensing*, 20(3), 1–9. https://doi.org/10.1080/014311699213280.

Fadlillah L.N., Sunarto., Widyastuti M., Marfai M.A. (2018). The impact of human activities in the Wulan Delta Estuary, Indonesia. *IOP Conf. Ser: Earth Environ Sci*, 148, 012032. https://doi.org/10.1088/1755-1315/148/1/012032.

Fadlillah L.N., Widyastuti M., Geottongsong T., Sunarto, Marfai M.A. (2019). Hydrological Characteristics of Estuary in Wulan Delta in Demak Regency, Indonesia. *Water Resources*, 46, 832-843. https://doi.org/10.1134/S0097807819060101.

Ghorai D. and Mahapatra M. (2020). Extracting Shoreline from Satellite Imagery for GIS Analysis. *Remote Sensing in Earth Systems Sciences*, 3, 13–22. https://doi.org/10.1007/s41976-019-00030-w.

Maglione P., Parente C., Vallario A. (2017). Coastline extraction using high resolution WorldView-2 satellite imagery. *European Journal of Remote Sensing*, 47(1), 685-699. https://doi.org/10.5721/EuJRS20144739.

Marfai M.A., Almohammad H., Dey S., Susanto B., and King L. (2008). Coastal dynamic, and shoreline mapping: multi-sources spatial data analysis in Semarang Indonesia. *Environ Monit Assess*, 142, 297-308. https://doi.org/10.1007/s10661-007-9929-2.

Marfai M.A. (2014). Impact of sea level rise to coastal ecology: a case study on the northern part of Java Island, Indonesia. *Quaestiones Geographicae*, 33(1), 107–114. https://doi.org/10.2478/quageo-2014-0008.

Marfai M.A., Tyas D.W., Nugraha I., Ulya A.F., Riasasi, W. (2016). The Morphodynamics of Wulan Delta and its impact on the coastal community in Wedung Subdistrict, Demak Regency, Indonesia. *Journal of Environmental Protection*, 7. 60-71.

Marfai M.A., Ahmada B., Mutaqin B.W., Windayati R. (2020). Dive Resort Mapping and Network Analysis: Water Resources Management in Pemuteran Coastal Area, Bali Island, Indonesia. *Geographia Technica*. 15(2), 106-116. http://doi.org/10.21163/GT_2020.152.11.

Mujabar P.S. and Chandrasekar N. (2013). Shoreline change analysis along the coast between Kanyakumari and Tuticorin of India using remote sensing and GIS. *Arabian Journal of Geosciences*, 6, 647-664. https://doi.org/10.1007/s12517-011-0394-4.

Muskananfola M.R., Supriharyono, Febrianto S. 2020. Spatio-temporal analysis of shoreline change along the coast of Sayung Demak, Indonesia using Digital Shoreline Analysis System. *Regional Studies in Marine Science*, 34, 101060. https://doi.org/10.1016/j.rsma.2020.101060.

Mutaqin B.W. (2017), Shoreline Changes Analysis in Kuwaru Coastal Area, Yogyakarta, Indonesia: An Application of the Digital Shoreline Analysis System (DSAS). *International Journal of Sustainable Development and Planning* 12(7), 1203-1214. https://doi.org/10.2495/SDP-V12-N7-1203-1214.

Mutaqin B.W., Lavigne F., Hadmoko D.S., Malawani M.N. (2019), Volcanic Eruption-Induced Tsunami in Indonesia: A Review, *IOP Conf. Ser.: Earth Environ. Sci*. 256 012023. https://doi.org/10.1088/1755-1315/256/1/012023.

Mutaqin B.W. (2020). Spatial Analysis and Geomorphic Characteristics of Coral Reefs on the Eastern Part of Lombok, Indonesia. *Geographia Technica*. 15(2), 202-211. http://doi.org/10.21163/GT_2020.152.19.

Mutaqin B.W., Marfai M.A., Helmi M., Rindarjono M.G., Windayati R., Sunarto (2020), Spatio-temporal Mapping of Ecotourism Activities in Buleleng Conservation Zone: A Methodological Review, *IOP Conf. Ser.: Earth Environ. Sci*. 451 012095. https://doi.org/10.1088/1755-1315/451/1/012095.

Nassar K., Fath H., Mahmod W.E., Masria A., Nadaoka K., Negm A. (2018). Automatic detection of shoreline change: case of North Sinai coast, Egypt. *Journal of Coastal Conservation*, 22, 1057–1083. https://doi.org/10.1007/s11852-018-0613-1.

Pardo-Pascual J.E., Sanchez-Garcia E., Almonacid-Caballer J., Palomar-Vazquez J.M., de los Santos E.P., Fernandez-Sarria A., and Balaguer-Beser A. 2018. Assessing the Accuracy of Automatically Extracted Shorelines on Microtidal Beaches from Landsat 7, Landsat 8 and Sentinel-2 Imagery. *Remote Sensing*, 10(2), 326. https://doi.org/10.3390/rs10020326.

Ruswanto and Adisaputra K. (1990). *Perkembangan Garis Pantai Welahan–Jepara Jawa Tengah*. Geologi Indonesia: Bandung.

Setiawan M.A., Rahayu E., and Sulistyaningrum Y. (2014). Dinamika Lingkungan Daerah Aliran Sungai dan Pesisir. In Sunarto, Marfai M.A., Setiawan M.A. *Geomorfologi dan Dinamika Pesisir Jepara*. 77-116. Yogyakarta: Gadjah Mada University Press.

Sunarto. (2005). Perubahan Fenomena Geomorfik Daerah Kepesisiran di Sekeliling Gunungapi Muria Jawa Tengah. *Dissertation*. Yogyakarta: Fakultas Geografi UGM.

Tong S.S., Pham T.L., Gunasekara K., Nguyen T.N., and Deroin J.P. (2014). Monitoring Coastal Morphological Changes Using Remote Sensing and GIS in the Red River Delta Area, Vietnam. *Photo Interpretation European Journal of Applied Remote Sensing*, 2, 51-97.

UNISDR/UNDP. (2012). *A Toolkit for Integrating Disaster Risk Reduction and Climate Change Adaption into Ecosystem Management of Coastal and Marine Areas in South Asia*. New Delhi: UNDP.

Wahyunto, Djohar H.H., and Marsoedi D.S. (1995). Analisis Data Penginderaan Jauh untuk Mendukung Identifikasi dan Inventarisasi Lahan Sawah di Daerah Jawa Barat. In Pusat Penelitian Tanah dan Agroklimat, Bogor (Eds.) *Proceedings of Pertemuan Teknis Penelitian Tanah dan Agroklimat*. 37-49.

Wicaksono A. and Wicaksono P. (2019). Geometric Accuracy Assessment for Shoreline Derived from NDWI, MNDWI, and AWEI Transformation on Various Coastal Physical Typology in Jepara Regency using Landsat 8 OLI Imagery in 2018. *Geoplanning J. Geomat. Plan*. 6(1), 55–72. https://doi.org/10.14710/geoplanning.6.1.55-72.

Zhang, Y. (2011). Coastal Environmental Monitoring Using Remotely Sensed Data and GIS Techniques in the Modern Yellow River Delta, China. *Environ Monit Assess*, 179(1-4), 15-29. https://doi.org/10.1007/s10661-010-1716-9.

Zhang Y. and Hou X. (2020). Characteristics of Coastline Changes on Southeast Asia Islands from 2000 to 2015. *Remote Sensing.* 12(3), 519. https://doi.org/10.3390/rs12030519.